Heat Transfer and Reaction in Laminar Tube Flow

R. I. ROTHENBERG and J. M. SMITH

University of California, Davis, California

An analytical study was made of the temperature and composition distribution and heat transfer characteristics for a reacting fluid in a tube. The reaction was assumed to be first order and irreversible and the flow to be laminar.

The results, which consisted of radial and axial profiles of temperature, composition, and Nusselt number could be expressed in terms of four parameters. The gradient of radial composition was usually sufficient to judge the effect of reaction on the heat transfer coefficient. Owing to residence time and temperature effects, the Nusselt number even for an exothermic reaction was usually greater than that for an inert system. For endothermic cases, the energy flux due to diffusion increases the total energy flow, and the Nusselt number may be several fold that in the corresponding nonreactive system.

For certain values of the parameters the radial temperature and composition profiles showed maxima and minima between the wall and center of the tube. At these conditions the direction of the flow of energy due to diffusion could not explain the increase in Nusselt number.

A first-order homogeneous reaction was studied under nonisothermal conditions in a laminar flow, tubular reactor. Owing to the radial temperature gradient, there is a variation in the reaction rate constant k_r across the tube. Also a radial variation in reaction time (residence time) exists due to the parabolic mass velocity profile. Both effects cause the extent of reaction to vary in the radial direction. This results in a radial composition gradient which in turn induces diffusion. The first objective was to determine radial and axial composition and temperature profiles under the combined influence of reaction kinetics, mass velocity distribution, heat, and mass transfer. Because of the large number of variables, some assumptions are necessary to obtain a solution. First the restriction to laminar flow means that radial transfer is solely by conduction. The omission of natural convection would significantly influence the results at some conditions. The experimental work of Colburn (*7*) and theoretical studies of Hsu and Smith (*10*) indicate that for inert systems the natural convection effect is less than 15% when the Grashof number does not exceed 1,000. This is an approximate statement because the effect is influenced by the Reynolds number (*13*). This criterion might also be used for reaction systems in the absence of a better approach. The Grashof number for the conditions of this paper is proportional to the cube of the ratio R/T_o. Hence natural convection would increase rapidly as the tube diameter increases and the temperature level decreases. Other assumptions are discussed later.

The counter diffusion of reactants and products results in an energy transfer radially. Therefore, the total energy flow is the sum of that due to the temperature and concentration gradients. Interpreted in terms of a total heat transfer coefficient, the results show that reaction can increase h several fold over that for an equivalent inert system. One of the objectives was to evaluate this increase as a function of the rate constants and enthalpy change of the reaction.

Cleland and Wilhelm (*5, 6*) solved the isothermal problem for laminar flow in a tubular reactor. Fuller (*8*) studied reaction under nonisothermal conditions for turbulent flow of a liquid. There have been numerous investigations (*3, 11, 15*) of the effect of an equilibrium reaction on heat transfer in turbulent flow. Also Brian and Reid (*1*) developed a method of predicting the increase in heat transfer coefficient due to reaction in turbulent flow. Their method is based upon film theory and assumes that the temperature gradient is small. To the authors' knowledge temperature and concentration profiles, or heat transfer coefficients, have not been studied for laminar flow in a tubular reactor.

THEORETICAL DEVELOPMENT

The reaction is assumed to be first order and irreversible. Also the molal diffusion fluxes of the reactants and products in the radial direction are assumed to be determined by the stoichiometry of the reaction. For example, for $aA \rightarrow bB$, $N_B = -b/a\, N_A$. Then the radial velocity and net radial mass flux can be shown to be zero. It then follows (Appendix) that the axial mass velocity in the nonisothermal fluid is given by

$$(\rho v_z) = 2\,G\,[1 - (r/R)^2] \qquad (1)$$

provided that constant density, laminar flow exists at the entrance to the reaction zone. Equation (1) reduces to the Poiseuille equation for constant density. Viscosity variation across the tube radius, due to temperature gradients, can distort the parabolic profile of Equation (1). This effect would be small for gaseous reactions in most instances but could be significant for liquid systems with large radial temperature variations. It also may be noted that Equation (1) also is based upon incompressible flow. In the laminar range this is probably a good assumption.

The assumption of stoichiometric diffusion fluxes is the basis for Equations (3) and (8) as well as (1). Its validity cannot be easily proven for a nonisothermal reaction system. It is the usual assumption made in considering reaction and flow in a tube with temperature variations (*2, 9, 11, 18*).

The following equations [to Equation (26)] are based upon an ideal gas mixture. Then the changes necessary to apply the results to a liquid reaction mixture are considered. The expression for the constant pressure diffusion of component A in a binary system is given by Bird, Stewart, and Lightfoot (*1*) as

$$N_A = y_A (N_A + N_B) - c D_{AB} \frac{\delta y_A}{\delta r} \qquad (2)$$

If A and B are reactant and product in the flowing reaction mixture, the above expression gives the radial diffusion rate of reactant. Using the assumption of stoichiometric diffusion, one can write Equation (2) as

$$N_A = - (cD_A) \frac{\delta y_A}{\delta r} \qquad (3)$$

where D_A, for the reaction $aA \rightarrow bB$, is

$$D_A = \frac{D_{AB}}{1 + \left(\frac{b}{a} - 1\right) y_A} \qquad (4)$$

in terms of the binary diffusivity D_{AB}.

The radial heat transfer contribution due to the temperature gradient is

$$q = - k \frac{\delta T}{\delta r} \qquad (5)$$

In combining these rate expressions [Equations (5) and (4)] with the conservation equations the following assumptions are made:

1. Variations in cD_A and the average molecular weight M have a negligible effect. The total molal concentration is a function of temperature ($c = P_T/R_gT$), and D_A is, in general, a function of composition and the binary diffusivities. For isothermal equal-molal counter diffusion, Equation (4) shows that $cD_A = cD_{AB}$. Hence for this case both cD_{AB} and M are constant. For nonisothermal diffusion cD_A is proportional to $T^{n/2}$, so that the effect of temperature variations is small. The influence of composition depends upon the system. For a reaction of the type $A \rightarrow 2B$, $cD_A = cD_{AB}/(1 + y_A)$. Also M will vary. In dilute systems where a large fraction of the gas is inert the variation in cD_A and M would be small.

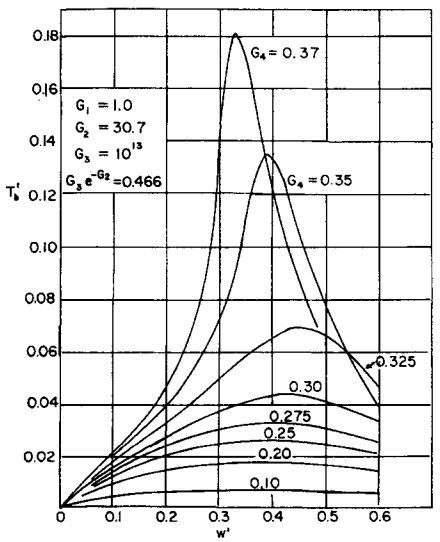

Fig. 1. Effect of heat of reaction (exothermic) on axial temperature profiles.

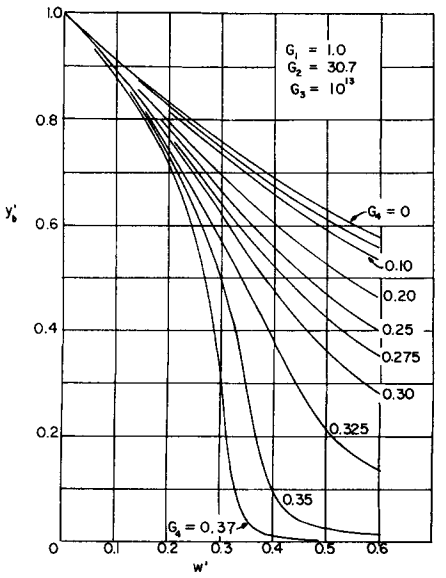

Fig. 2. Effect of heat of reaction (exothermic) on axial composition profiles.

2. k, C_p, ΔH, and P_T are constant.
3. Kinetic energy and gravitation effects are negligible.
4. Axial mass and energy transfer are negligible.

Conservation Equations

With the stated assumptions the mass balance of A is

$$- \frac{\delta (rN_A)}{r\,\delta r} - R_A = (\rho v_z) \frac{\delta (y_A/M)}{\delta z} \qquad (6)$$

where y_A/M is the molal concentration of A per unit mass, and R_A is the rate of disappearance of A due to reaction.

The enthalpy balance must account for the energy change due to the reaction. It is convenient first to develop an expression for the enthalpy of the system at any point. This can be expressed as a linear function of T and y_A/M; that is

$$H - H_o = C_p (T - T_o) - \Delta H[(y_A/M) - (y_A/M)_o] \qquad (7)$$

where H_o is the reference enthalpy at T_o and y_{A_o} (the entrance condition).

The radial flux of energy due to diffusion is $\Sigma N_i \tilde{H}_i$. From the assumption of stoichiometric diffusion

$$\Sigma N_i \tilde{H}_i = - N_A \Delta H \qquad (8)$$

Now an energy balance can be written including the radial contributions due to heat conduction and mass diffusion and the change in enthalpy due to flow in the axial direction. From Equations (7) and (8) this is

$$\Delta H \frac{\delta (r N_A)}{r\,\delta r} - \frac{\delta (rq)}{r\,\delta r} = \rho V_z \left[C_p \frac{\delta T}{\delta z} - \Delta H \frac{\delta (y_A/M)}{\delta z} \right] \qquad (9)$$

This can be stated in a simpler form by combination with the mass balance [Equation (4)]:

$$- \frac{\delta (rq)}{r\,\delta r} - (\Delta H) R_A = (\rho V_z) C_p \frac{\delta T}{\delta z} \qquad (10)$$

For the gaseous reaction

$$R_A = k_r p_A = A_g \left[\exp\left(- \frac{E}{R_g T} \right) \right] p_A \qquad (11)$$

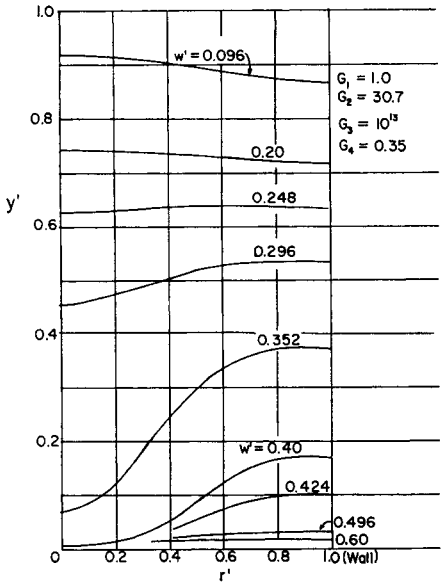

Fig. 3. Radial composition profiles for exothermic reactions.

For boundary conditions the wall and inlet temperatures were chosen to be equal constants, and the inlet composition was taken as y_{A_o}. Hence

$$T = T_o,\ y = y_{A_o} \text{ at } z = 0 \tag{12}$$

$$T = T_o \text{ at } r = R \tag{13}$$

and because of the wall restriction

$$\frac{\delta y_A}{\delta r} = 0 \text{ at } r = R \tag{14}$$

If Equations (1), (5), (3), and (9) are substituted in Equations (6) and (10), the conservation equations are obtained in terms of the primary variables r, z, y_A, and T. Dimensionless forms of these two expressions along with definitions of the dimensionless variables are given below:

$$\frac{\delta y'}{\delta w'} = \frac{G_1}{1-(r')^2}\left[\frac{1}{r'}\frac{\delta y'}{\delta r'} + \frac{\delta^2 y'}{(\delta r')^2}\right] - \frac{G_3}{1-(r')^2} y' \exp\left(-\frac{G_2}{T'+1}\right) \tag{15}$$

$$\frac{\delta T'}{\delta w'} = \frac{1}{1-(r')^2}\left[\frac{1}{r'}\frac{\delta T'}{\delta r'} + \frac{\delta^2 T'}{(\delta r')^2}\right] + \frac{G_3 G_4}{1-(r')^2} y' \exp\left(-\frac{G_2}{T'+1}\right) \tag{16}$$

$$r' = r/R \tag{17}$$

$$w' = \frac{z}{R\, N_{Re}\, N_{Pr.}} = \frac{k}{2R^2\, G\, C_p} z \tag{18}$$

$$y' = y_A/y_{A_o} \tag{19}$$

$$T' = \frac{T - T_o}{T_o} \tag{20}$$

The G parameters necessary in Equations (15) and (16) are the following dimensionless assemblies of the properties of the system:

$$G_1 = \text{Lewis number} = \frac{C_p\, Mc\, D_A}{k} \tag{21}$$

$$G_2 = \text{activation energy group} = \frac{E}{R_g\, T_o} \tag{22}$$

$$G_3 = \text{frequency factor group} = \frac{R^2\, MC_p\, P_T\, A_g}{k} \tag{23}$$

$$G_4 = \text{heat of reaction group} = -\frac{(\Delta H) y_{A_o}}{M\, C_p\, T_o} \tag{24}$$

Finally the boundary conditions in dimensionless form are

$$T' = 0,\ y' = 1 \text{ at } w' = 0 \tag{25}$$

$$T' = 0,\ \frac{\delta y'}{\delta r'} = 0 \text{ at } r' = 1 \tag{26}$$

Adaptation to Liquid Reaction System

Equations identical in form to (15) and (16) can be derived for reaction in a constant density liquid, provided that R_A is given by

$$R_A = k_{rL}\, c_A = (A_L\, e^{-E_L/R_g T})\, c_A \tag{27}$$

In this case, $y' = c_A/c_{A_o}$, and the dimensionless groups are defined as $G_1 = C_p\, \rho\, D_A/k$, $G_3 = R^2\, \rho\, C_p\, A_L/k$, and $G_4 = -\Delta H\, c_{A_o}/T_o\, \rho\, C_p$. The equation of G_2 is the same as Equation (22). It may be noted that for a liquid system Equation (2) becomes $N_A = -D_A\, (\delta c_A)/(\delta r)$, and Equation (7) takes the form $H - H_o = C_p\, (T - T_o) - \Delta H[(c_A/\rho) - (c_{A_o}/\rho)]$.

METHOD OF SOLUTION

The solution of coupled and nonlinear Equations (15) and (16) gives the temperature and composition at any point in the tube. From these results the heat transfer characteristics can be derived. Solutions were obtained by finite difference techniques by machine computation. The equations and derived quantities are summarized.

Derived Quantities

Bulk Values. The bulk temperature and composition result when the fluid at a given axial position is mixed at constant enthalpy and no further reaction occurs. With this definition, the equations for T_b' and y_b' can be expressed as follows:

$$T_b' = 4\int_0^1 T'\,[r' - (r')^3]\, dr' \tag{28}$$

$$y_b' = 4\int_0^1 y'\,[r' - (r')^3]\, dr' \tag{29}$$

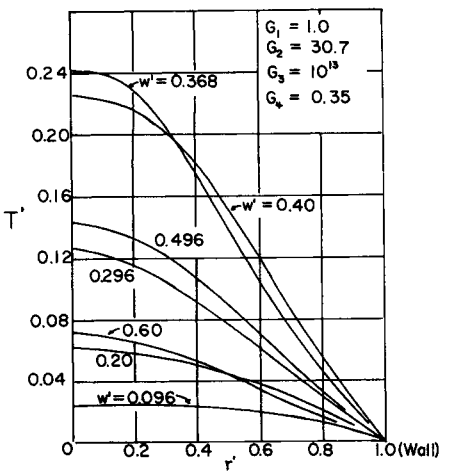

Fig. 4. Radial temperature profiles for exothermic reactions.

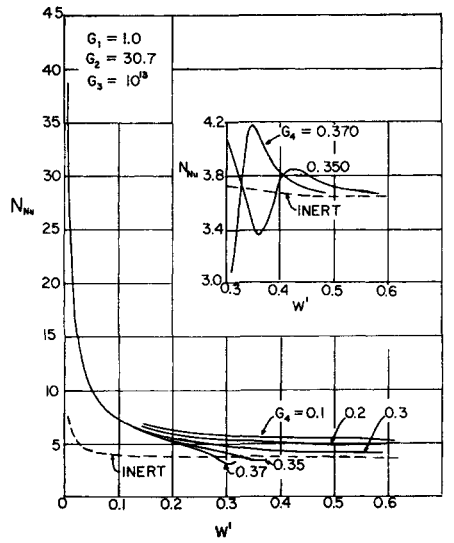

Fig. 5. Point Nusselt numbers for exothermic reactions.

Point Nusselt Number. The Nusselt number indirectly includes the energy flux due to diffusion. Thus the heat transfer coefficient used in formulating N_{Nu} is the total wall energy flux divided by $T_b - T_o$. The point value can be shown to be

$$N_{Nu} = \frac{q_w(2R)}{kT_o}\left(\frac{1}{T_b'}\right) \tag{30}$$

The finite difference expression used to evaluate q_w, the total wall energy flux, is given by Equation (38).

Average Nusselt Number. The average Nusselt number over the reactor length 0 to z was based upon an arithmetic mean temperature difference (A logarithmic value was not possible since $T_b = T_o$ at the tube entrance). Hence

$$N_{Nu_a} = \frac{Q}{(\pi z)(T_b - T_o)_a k} = \frac{2Q}{\pi z (T_b - T_o)_z k} \tag{31}$$

The heat transfer rate from 0 to z is

$$Q = \pi R^2 G[H_o - (H_b)_z] \tag{32}$$

Combining Equations (31), (32), and (7), and introducing dimensionless variables, one gets the following expression for N_{Nu_a}:

$$N_{Nu_a} = \frac{1}{w'}\left[-1 + \frac{G_4(1 - y_b')}{T_b'}\right] \tag{33}$$

where T_b' and y_b' are evaluated at w'.

Finite Difference Equations

The derivatives in Equations (15) and (16) can be replaced by difference approximations. If subscripts n and j represent radial and axial increments, the temperature form of the difference equations are

$$\frac{\delta T}{\delta z} = \frac{T_{n,j+1} - T_{n,j}}{\Delta z} \tag{34}$$

$$\frac{\delta T}{\delta r} = \frac{1}{2}\left[\frac{T_{n+1,j+1} - T_{n-1,j+1}}{2\Delta r} + \frac{T_{n+1,j} - T_{n-1,j}}{2\Delta r}\right] \tag{35}$$

$$\frac{\delta^2 T}{\delta r^2} = \frac{1}{2}\left[\frac{T_{n+1,j+1} - 2T_{n,j+1} + T_{n-1,j+1}}{\Delta r^2} + \frac{T_{n+1,j} - 2T_{n,j} + T_{n-1,j}}{\Delta r^2}\right] \tag{36}$$

Analogous expressions were used for y_A

The rate term for the axial increment was evaluated at the temperature and concentration at the beginning of the increment.

With these approximations two sets of equations are generated: one for $y'_{n,j+1}$ and one for $T'_{n,j+1}$. Modifications are required for the center of the tube as presented in reference *19*. The procedure used for numerical solution is similar to that described by Bruce et al. (*4*) and by Lapidus (*16*).

A special technique was employed at the tube wall to relate $y'_{w,j+1}$ and $y'_{w-1,j+1}$. A mass balance for a cylindrical element bounded by R and $R - (\Delta r/2)$ gives

$$\frac{y'_{w,j+1} - y'_{w-1,j+1}}{\Delta r'} = -\frac{G_8}{2G_1}(y'_{w,j+1})\,\Delta r'\, e^{-G_2} \tag{37}$$

In this particular balance axial flow is neglected. A similar expression was used by Cleland (5). It reduces to $\delta y'/\delta r' = 0$ as $\Delta r'$ approaches zero.

Equation (37) is the finite difference analogy of the boundary condition represented by part of Equation (26).

The expression for q_w, needed to evaluate the Nusselt number [Equation (30)], was derived in a similar fashion from an enthalpy balance at the wall. The result corresponding to axial location $(j+1)$ is

$$q_w R = \frac{R - \Delta r/2}{\Delta r}\{-k(T_{w,j+1} - T_{w-1,j+1}) + \Delta H c\, D_A[y_{Aw,j+1} - y_{Aw-1,j+1}]\} \tag{38}$$

A check was included in the computer program to indicate errors. The average of the wall fluxes at the beginning and the end of each axial increment was compared with the enthalpy change of the fluid flowing through the element. This is expressed by

$$\frac{(q_w)_j + (q_w)_{j+1}}{2} = -\frac{RG}{2\Delta z}(H_{b,j+1} - H_{b,j}) \tag{39}$$

In the final results, the two sides of Equation (39) were in excellent agreement, except for the first few axial increments. For example, for the $G_4 = 0.35$ run shown in Figures 1 and 2, the difference between the two sides was 6% at $w' = 0.008$, decreased to 1% at $w' = 0.100$, and was less than 1% at higher axial distances.

RESULTS

Numerical data were obtained to show the effects of heat of reaction for exothermic and endothermic systems,

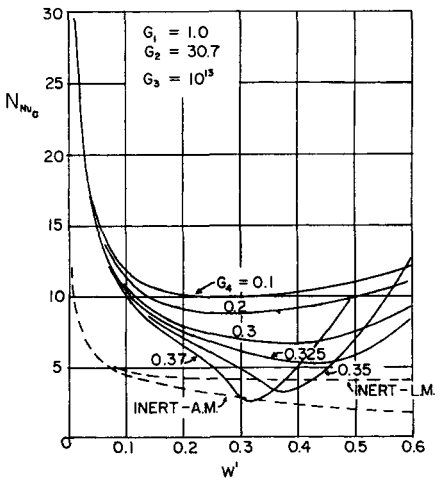

Fig. 6. Average Nusselt numbers for exothermic reactions.

the rate of reaction (frequency factor and activation energy), and the Lewis number. For each set of parameters (G_1 to G_4) the data consisted of radial and axial profiles of temperature and mole fraction y_A and point and average Nusselt numbers. The latter results were compared with a Nusselt number for a corresponding inert system. The inert result is based upon constant and unequal wall and entrance temperatures (the Graetz-Nusselt problem), and the solution is discussed in several references (*12, 14, 17*).

Only a few figures illustrating the data are presented. Complete results are given in reference *19*.

Heat of Reaction (Exothermic)

In this series G_1, G_2, and G_3 were chosen to represent a more or less typical gaseous reaction system, and G_4 was varied. Thus for gases the Lewis number (G_1) is usually close to unity; $G_3 = 10^{13}$ corresponds roughly to a frequency factor of 10^{13} sec.$^{-1}$; and G_2 is 30.7 when the activation energy is 30,700 cal./g. mole at 500°K. or 15,350 cal./g. mole at 1,000°K.

Figures 1 and 2 show the bulk temperature and composition vs. reactor length. Figure 1 indicates that the distance of the maximum temperature from the reactor inlet first increases and then decreases as the heat of reaction increases. The peak becomes sharper as G_4 increases, and it was difficult to obtain a stable computer solution for $G_4 > 0.370$.

The mole fraction of reactant decreases more rapidly the higher the heat of reaction, as noted by the increasingly steep slopes of the curves in Figure 2. For $G_4 = 0.370$ the reaction is essentially complete at $w' = 0.5$. The upper curve for $G_4 = 0$ represents isothermal conditions and agrees well with the results of Cleland (5). In fact for these values of G_1, G_2, and G_3 the effect of residence time distribution in a laminar, isothermal reactor is small. Hence, the upper curve is almost the same as that for plug-flow conditions. In the latter situation y_b' is given by

$$y_b' = \exp(-2k_o'w') \qquad (40)$$

where k_o is a dimensionless rate constant given by

$$k_o' = G_3 \exp(-G_2) \qquad (41)$$

The key to explaining the heat transfer characteristics in a reacting system are the radial profiles. Figures 3 and 4 show these results for the $G_4 = 0.350$ curves of Figures 1 and 2. For these conditions reaction becomes nearly

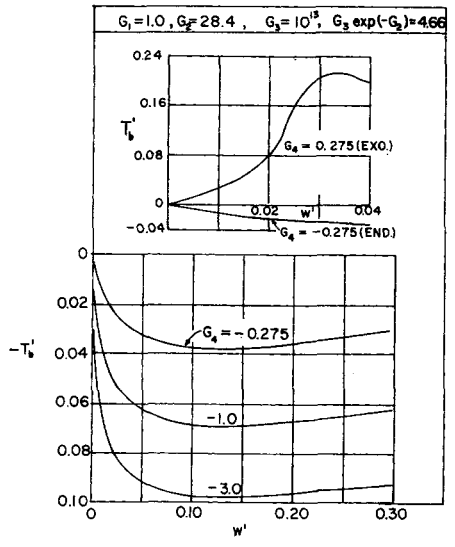

Fig. 7. Axial temperature profiles for endothermic reactions.

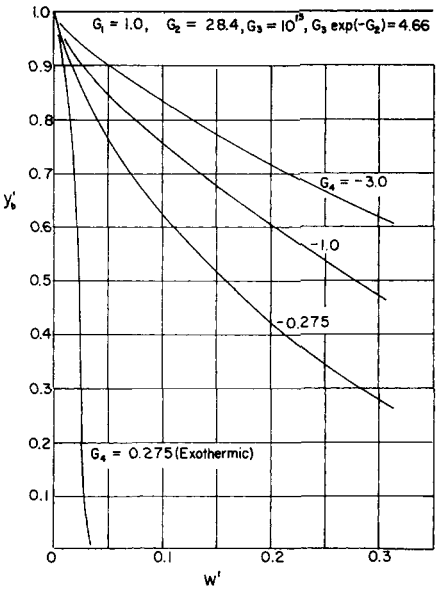

Fig. 8. Axial composition profiles for endothermic reactions.

complete at $w' = 0.6$ (Figure 2). In an exothermic system the energy transfer due to the temperature difference is usually directed toward the wall, as illustrated in Figure 4. Because of the higher temperatures near the center of the tube, it would be expected that the mole fraction of A would be less at this location. Figure 3 verifies this for $w' \geq 0.296$. In this region A diffuses away from the wall. Since the reaction is exothermic, the energy transfer due to diffusion is also directed away from the wall, or opposite to the energy flux due to the temperature gradient. Hence for $w' \geq 0.296$ it is expected that the total (net) energy flux could be less than that for an inert system. Figure 5 shows the point Nusselt number vs. w' for the same conditions as Figure 1 and 2. It is noted that N_{Nu} for $G_4 = 0.35$ does dip below the inert curve at w' somewhat greater than 0.3. This is more clearly seen on the insert plot.

For $w' \leq 0.296$, Figure 3 shows that the energy flow near the wall due to diffusion will be directed toward the wall, augmenting the energy transfer due to the temperature gradient. Hence N_{Nu} should be greater than that for an inert system, and this is confirmed by the curve in Figure 5 for $G_4 = 0.350$.

For $G_4 < 0.35$, the radial composition profiles usually fall in the wall direction so that the energy flux due to diffusion increases the total energy flow. Accordingly, for low G_4 the Nusselt number is greater than the inert result (Figure 5).

The drop in composition near the wall for $w' < 0.296$ (Figure 3) is due to the lower velocity and longer reaction time at this location. At low axial distances the temperature at the center is not much greater than that at the wall, for example, see the curve for $w' = 0.096$ in Figure 4. Therefore, the increased rate of reaction at the center is more than balanced by the longer reaction time near the wall, and more reactant is consumed in the latter location. This effect becomes more pronounced as the heat of reaction decreases and explains the increase in Nusselt number shown in Figure 5 with decreasing G_4. These results demonstrate that the distribution of residence times in laminar flow can have a significant effect on the heat transfer characteristics of a nonisothermal system. For a plug-flow reactor (uniform velocity profile and constant residence time) in which mass and heat transfer are by molecular diffusion and conduction, y_A

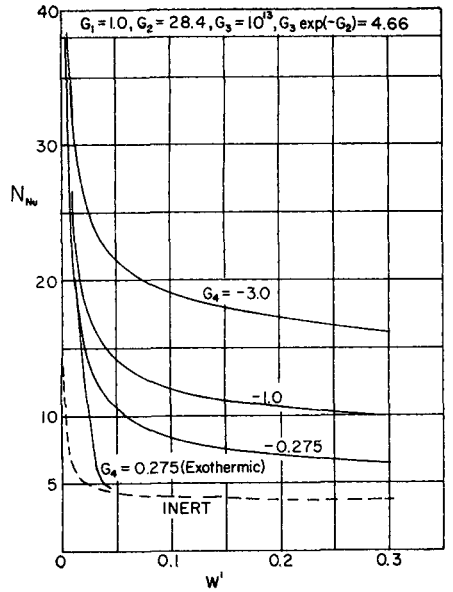

Fig. 9. Point Nusselt numbers for endothermic reactions.

would be higher near the wall than at the center. Here the Nusselt number likely would be less than that for an inert system. The opposite situation in Figure 5 is due to the longer residence time near the wall.

The actual value of N_{Nu} depends upon the temperature gradient at the wall and the bulk temperature, and these quantities in turn are influenced by flow, diffusion, heat transfer, and the reaction kinetics. Hence a simple explanation such as presented is not exact. However, the trend of the curves in Figure 5 can be explained by the direction of the radial gradient of composition. It may be noted that exact correspondence between inert and reaction N_{Nu} curves would not be expected, regardless of the energy contribution due to diffusion. This is because the boundary conditions for the two situations are not comparable. The inert result is based upon constant and unequal wall and inlet temperatures, while for the reaction case these temperatures are the same.

The radial profiles in Figures 3 and 4 were found to represent the normal results. For other values of G_1 to G_3, unusual profiles may occur. These are discussed later.

In Figure 6 average Nusselt numbers are shown for the same operating conditions. In the inert case, the fluid entering the reactor and the wall are at different temperatures so that Nusselt numbers based upon either arithmetic or log-mean temperature differences can be used. Hence two inert curves are given in Figure 6. The comparison with the arithmetic mean curve is of limited value because of the different boundary conditions. For example, the inert curve approaches zero as w' increases, while the reaction curves approach indeterminate values. This is discussed more fully in reference *19*.

Heat of Reaction (Endothermic)

Here the temperature increases from the center toward the wall of the tube. The higher temperature and increased residence time augment each other in causing y_A to decrease in the wall direction. Because the energy flux is opposite to the direction of diffusion of A for an endothermic system, the diffusive energy contribution is toward the center. Thus both contributions to the total energy transfer supplement each other, leading to Nusselt numbers considerably larger than for the inert system.

Figures 7, 8, and 9 illustrate the effect of negative values of G_4 on T_b', y_b', and N_{Nu} for constant G_1, G_2, and G_3. The results for an exothermic run at the same G_1, G_2, and G_3 are also included. The comparison of the curves (Figure 9) for $G_4 = \pm 0.275$ indicates the large effect of the direction of the diffusive energy flow.

Rate of Reaction

Equations (15) and (16) show that the influence of the rate of reaction is determined by $G_3 \exp(-G_2)$. Increasing the rate by either increasing G_3 (proportional to the frequency factor) or decreasing G_2 (proportional to activation energy) have similar effects on the axial plots of T_b', y_b', or N_{Nu}. For an exothermic reaction, an increase in rate raises the level of the maximum T_b' and moves it toward the reactor inlet. Also the point Nusselt number approaches the inert curve at a lower w' the higher the rate of reaction.

However, changing the rate constant (k_o') can have a decided effect on the radial profiles. A striking example results when the activation energy is changed so as to increase the initial rate constant tenfold. For example, if G_1 and G_3 are the same as in Figures 3 and 4 but G_2 is reduced to 28.4, the radial profiles for $G_4 = +0.275$ are as shown in Figures 10 and 11. The axial profiles for these new conditions are those given by the exothermic curve in Figures 7 to 9. They are of the same shape as those in Figures 3 to 5 for the higher activation energy. In contrast, the radial profiles show maxima and minima at intermediate r and in general are substantially different from those of Figures 3 and 4. As might be expected, these unusual profiles have an effect on the heat transfer coefficient and N_{Nu}. To analyze this it is first necessary to investigate the reasons for the maxima and minima.

First, it is noted from Figure 8 that the reaction is essentially complete at $w' \geq 0.035$. The fall in y_A near the wall for low w' (Figure 11) is due to the combined effect of residence time and temperature as described previously. This causes an energy flux toward the wall due to diffusion. Right at the wall the composition gradient must be zero. Hence the extra energy due to diffusion is transferred at the wall by an increased temperature gradient. In contrast, the composition is essentially uniform near the center of the tube so that there is a negligible energy flux because of diffusion. These two effects result in a maximum in the temperature profile, as observed in Figure 10. At low w' this maximum is not very significant;

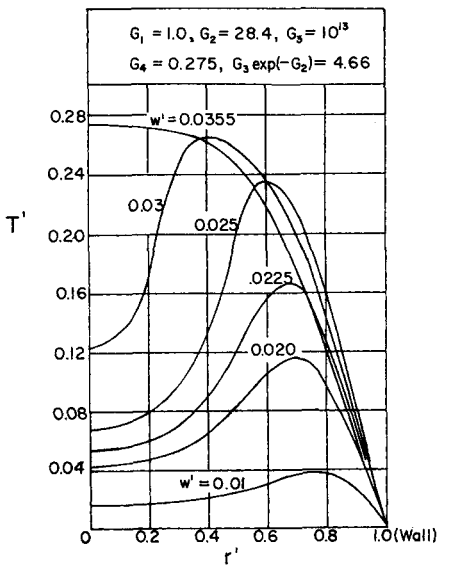

Fig. 10. Radial temperature profiles for high reaction rate.

for example, note the curve for $w' = 0.01$. However, the increased temperature increases the reaction rate. This further reduces y_A and increases the wall directed energy flux due to diffusion. Hence as w' increases, the temperature maximum in Figure 10 becomes more significant, and simultaneously a composition minimum develops (see Figure 11). This situation continues until finally y_A becomes nearly zero at r' corresponding approximately to those for the maxima T'. The decrease in y_A offsets the temperature effect, and the rate of reaction and heat evolved decrease. Hence, the temperature near the wall actually falls slightly (crossing of curves in Figure 10), and the maximum T' is shifted toward the center of the tube. When $w' = 0.0355$, the reaction is complete, and the temperature profile approaches that of a cooling curve with a maximum at the center.

At $w' = 0.025$, Figure 11 shows that the energy flux due to diffusion is directed toward the center for r' greater than 0.7. The total energy transfer in this exothermic system is reduced by the diffusion contribution. Despite this, reference to Figure 9 indicates that the Nusselt number for reaction at this w' is about twice that for an inert system. The explanation is found in the radial temperature profile. The heat transfer coefficient is given by

$$h = \frac{-k(\delta T/\delta r)_w}{(T_b - T_o)} \tag{42}$$

and

$$N_{Nu} = \frac{-2R(\delta T/\delta r)_w}{(T_b - T_o)} \tag{43}$$

The profile in Figure 10 at $w' = 0.025$ shows a large wall gradient and suggests a low T_b. As Equation (43) indicates, both of these factors cause a large Nusselt number. Here is a case where the heat transfer coefficient is increased significantly above the inert value when the energy flux due to diffusion opposes the energy flow caused by the temperature gradient.

Lewis Number

The previous results were all restricted to a Lewis number of unity. For liquids, $G_1 = 0.001$ is more appropriate. Here the diffusivity is much less, and the system would behave somewhat like annular layers of fluid which were separated by impermeable membranes. The results are illustrated for an exothermic reaction in Figure

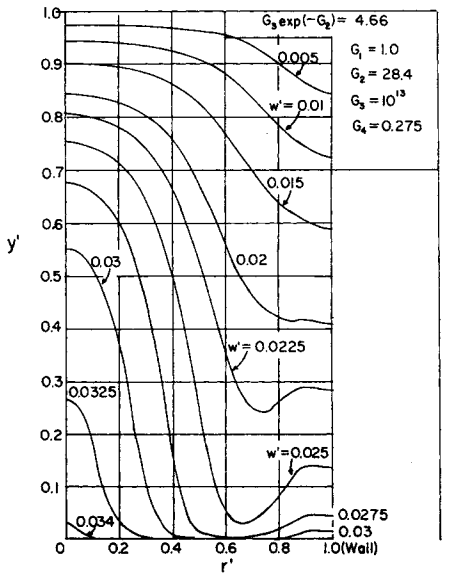

Fig. 11. Radial composition profiles for high reaction rate.

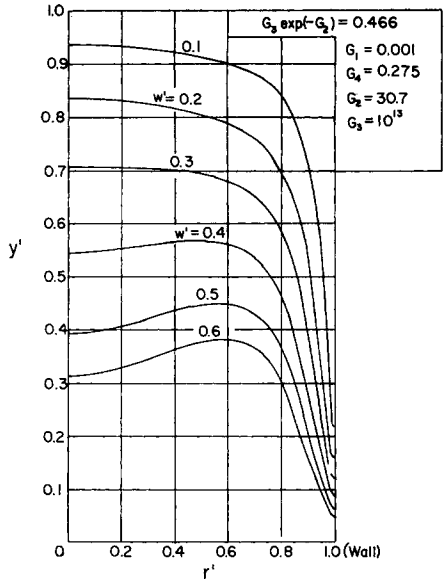

Fig. 12. Radial composition profiles for low Lewis number.

12. The composition gradients are large, and y' is lower at the wall than at the center. Again the reduction near the wall is caused by the longer residence time for reaction. For the same G_2, G_3, and G_4 as listed on Figure 12, the chief effect of changes in Lewis number was on the radial profiles.

CONCLUSIONS

The radial composition profiles suggest that in laminar flow in a nonisothermal system the distribution of residence times can have a significant effect. This is also evident from the increase in Nusselt number due to reaction for an exothermic system.

The Nusselt number for reacting fluids is greater than for inert flow under most conditions for either exothermic or endothermic reactions. In general the effect can be related to the direction of the radial concentration gradient and therefore to the direction of the extra energy transfer due to diffusion. However, for some situations unusual radial profiles with unsymmetrical maxima or minima are observed. When this occurs, the increase in Nusselt number is not caused by an extra wall-directed energy flux. Rather the heat transfer coefficient is unusually high because of a steep temperature gradient at the wall combined with a relatively low bulk temperature.

ACKNOWLEDGMENT

The financial support of the National Science Foundation in the form of a Cooperative Graduate Fellowship is gratefully acknowledged.

The authors also express their appreciation to the University of California Computer Center at Davis and to the National Institutes of Health whose Grant No. FR-00009 made the computer facilities available.

NOTATION

A_g = frequency factor in Equation (11), g. mole/(sec.) (cc.) (atm.)
A_L = frequency factor in Equation (27), sec.$^{-1}$
c = total concentration, g. mole/cc.
C_p = specific heat of reaction mixture, cal./(g.) (°K.)
D_A = effective diffusivity of A in the reacting mixture, defined in Equation (4), sq. cm./sec.
E (or E_L) = activation energy, cal./g. mole

G = mass flow rate divided by the cross-sectional area of the tube, g./(sq. cm.)(sec.)
h = point heat transfer coefficient, cal./(sec.)(sq. cm.)(°K.)
H = enthalpy of the reaction mixture, cal./g.; $\widetilde{H}_i$ refers to the molal enthalpy of component i, cal./g. mole
ΔH = heat of reaction per mole of reactant A, cal./g. mole
k = thermal conductivity, cal./(sec.)(cm.)(°K.)
k_r = reaction rate constant in Equation (11), g. mole/(sec.)(cc.)(atm.)
k_{rL} = reaction rate constant in Equation (27)
k_o' = dimensionless rate constant defined by Equation (41)
M = average molecular weight of reacting mixture, g./g. mole
N_A = radial diffusion rate of A, g. mole/(sq. cm.)(sec.)
p_A = partial pressure of A, atm.
P_T = total pressure, atm.
q = point radial heat transfer rate, cal./(sq. cm.)(sec.)
q_w = heat transfer rate to the tube wall
Q = total heat transfer rate to the wall over reactor length z., cal./sec.
r = radial distance in wall direction, cm.
R = tube radius, cm.
r' = r/R
R_A = rate of disappearance of A due to reaction, g. mole/(cc.)(sec.)
R_g = gas constant
T = absolute temperature, °K.
T' = $(T - T_o)/T_o$
v_z = axial velocity, cm./sec.
y_A = mole fraction of A
y' = y_A/y_{A_o}
z = axial distance from reactor inlet, cm.
w' = dimensionless axial distance defined by Equation (18)
ρ = density of reaction mixture, g./cc.
(ρv_z) = axial mass velocity at any radius, g./(sq. cm.)(sec.)

Dimensionless Groups

G_1 to G_4 defined by Equations (21) to (24)
N_{Nu} = point Nusselt number; N_{Nu_a} = average Nusselt number based upon arithmetic average temperature difference
N_{Pr} = Prandtl number
N_{Re} = Reynolds number

Subscripts

A = component A
b = bulk mean value
j = axial increment number
n = radial increment number
o = inlet of reactor; this subscript also denotes wall temperature, since $T_o = T_w$
w = tube wall

LITERATURE CITED

1. Bird, R. B., W. E. Stewart, and E. N. Lightfoot, "Transport Phenomena," p. 502, Wiley, New York (1960).
2. Brian, P. L. T., and R. C. Reid, *A.I.Ch.E. Journal*, 8, 322 (1962).
3. Brokaw, R. S., *Natl. Advisory Comm. Aeronaut. RM E57K19a* (March 5, 1958).
4. Bruce, G. H., D. W. Peaceman, H. H. Rachford, Jr., and J. D. Rice, *Petrol. Trans. Am. Inst. Mining Engrs.*, 198, 79 (1953).
5. Cleland, F. A., Ph.D. thesis, Princeton Univ., Princeton, New Jersey (May, 1954); available from University Microfilms, Ann Arbor, Michigan.
6. ———, and R. H. Wilhelm, *A.I.Ch.E. Journal*, 2, 489 (1956).
7. Colburn, A. P., *Trans. Am. Inst. Chem. Engrs.*, 29, 174 (1933).
8. Fuller, O. M., Ph.D. thesis, Georgia Institute of Technology, Atlanta, Georgia (Jan., 1962).
9. Furgason, R. R., and J. M. Smith, *A.I.Ch.E. Journal*, 8, 654 (1962).
10. Hsu, Y.-Y., and J. M. Smith, *J. Heat Transfer*, Series C 83, 176 (1961).
11. Irving, J. P., and J. M. Smith, *A.I.Ch.E. Journal*, 7, 91 (1961).
12. Jakob, M., "Heat Transfer," Vol. 1, Wiley, New York (1949).
13. Kern, D. Q., and D. F. Othmer, *Trans. Am. Inst. Chem. Engrs.*, 39, 517 (1943).
14. Knudsen, J. G., and D. L. Katz, "Fluid Dynamics and Heat Transfer," McGraw-Hill, New York (1958).
15. Krieve, W. F., and D. M. Mason, *JPL Prog. Rep. 20-366* (Nov., 1958).
16. Lapidus, L., "Digital Computation for Chemical Engineers," McGraw-Hill, New York (1962).
17. Norris, R. H., and D. D. Streid, *Trans. Am. Soc. Mech. Engrs.*, 62, 525 (1940).
18. Richardson, J. L., F. P. Boynton, K. Y. Eng, and D. M. Mason, *Chem. Eng. Sci.*, 13, 130 (1961).
19. Rothenberg, R. I., Ph.D. thesis, Univ. of California, Davis, California (Sept., 1964), available from University Microfilms, Ann Arbor, Michigan.

APPENDIX: DERIVATION OF EQUATION (1)

Suppose the reaction is

$$aA \rightarrow bB$$

The assumption of stoichiometric diffusion means

$$N_B = -\frac{b}{a} N_A \qquad (A)$$

The radial velocity is given by

$$v_r = \frac{1}{\rho}(n_A + n_B) = \frac{1}{\rho}(M_A N_A + M_B N_B) \qquad (B)$$

where n_A and n_B are the mass diffusion fluxes (see Bird, Stewart, and Lightfoot, p. 498, Table 16.1-2,D). Since the molecular weights are related by $M_B = \frac{a}{b} M_A$, (conservation of mass), Equation (B) becomes

$$v_r = \frac{M_A}{\rho}\left(N_A + \frac{a}{b} N_B\right) \qquad (C)$$

Utilizing Equation (A) one obtains

$$v_r = 0 \qquad (D)$$

or the radial velocity (and mass velocity) is zero.

Next assume that the flow at the entrance to the reaction section is laminar. This means that at $w' = 0$, for incompressible, constant viscosity, flow

$$v_z = 2\bar{v}[1 - (r/R)^2] \qquad (E)$$

where $\bar{v}$ = the average velocity. If in addition the density is constant at $w' = 0$, Equation (E) becomes

$$(\rho v_z) = 2G[1-(r/R)^2] \qquad (F)$$

This expression applies at $w' = 0$. Now as the fluid enters the reaction zone ($w' > 0$), Equation (D) tells one that there can be no net mass transferred radially. Therefore, the axial mass flux will still be given by Equation (F), which is Equation (1), at any w'.

Manuscript received September 14, 1965; revision received January 8, 1965; paper accepted January 11, 1965. Paper presented at A.I.Ch.E. Dallas meeting.